DOI: 10.1002/chem.200500610

Host–Guest Interactions in the Supramolecular Incorporation of Fullerenes into Tailored Holes on Porphyrin-Modified Gold Nanoparticles in Molecular Photovoltaics

Hiroshi Imahori,*[a, b, c] Atsushi Fujimoto,[a] Soonchul Kang,[a] Hiroki Hotta,[b] Kaname Yoshida,[d] Tomokazu Umeyama,[a] Yoshihiro Matano,[a] Seiji Isoda,[d] Marja Isosomppi,[e] Nikolai V. Tkachenko,*[e] and Helge Lemmetyinen[e]

Abstract: Novel gold nanoparticles modified with a mixed self-assembled monolayer of porphyrin alkanethiol and short-chain alkanethiol were prepared (first step) to examine the size and shape effects of surface holes (host) on porphyrin-modified gold nanoparticles. The porphyrin-modified gold nanoparticles with a size of about 10 nm incorporated C_{60} molecules (guest) into the large, bucket-shaped holes, leading to the formation of a supramolecular complex of porphyrin–C_{60} composites (second step). Large composite clusters with a size of 200–400 nm were grown from the supramolecular complex of porphyrin–C_{60} composites in mixed solvents (third step) and deposited electrophoretically onto nanostructured SnO_2 electrodes (fourth step). Differences in the porphyrin:C_{60} ratio were found to affect the structures and photoelectrochemical properties of the composite clusters in mixed solvents as well as on the SnO_2 electrodes. The photoelectrochemical performance of a photoelectrochemical device consisting of SnO_2 electrodes modified with the porphyrin–C_{60} composites was enhanced relative to a reference system with small, wedged-shaped surface holes on the gold nanoparticle. Time-resolved transient absorption spectroscopy with fluorescence lifetime measurements suggest the occurrence of ultrafast electron transfer from the porphyrin excited singlet states to C_{60} or the formation of a partial charge-transfer state in the composite clusters of supramolecular complexes formed between porphyrin and C_{60} leading to efficient photocurrent generation in the system. Elucidation of the relationship between host–guest interactions and photoelectrochemical function in the present system will provide valuable information on the design of molecular devices and machines including molecular photovoltaics.

Keywords: donor–acceptor systems · fullerenes · host–guest systems · nanostructures · porphyrinoids · self-assembly

[a] Prof. H. Imahori, A. Fujimoto, S. Kang, Dr. T. Umeyama, Prof. Y. Matano
Department of Molecular Engineering
Graduate School of Engineering
Kyoto University, Nishikyo-ku, Kyoto 615-8510 (Japan)
Fax: (+81) 75-383-2571
E-mail: imahori@scl.kyoto-u.ac.jp

[b] Prof. H. Imahori, Dr. H. Hotta
PRESTO, JAPAN Science and Technology Agency (JST)
Nishikyo-ku, Kyoto 615-8510 (Japan)

[c] Prof. H. Imahori
Fukui Institute for Fundamental Chemistry, Kyoto University
34-4, Takano-Nishihiraki-cho, Sakyo-ku, Kyoto 606-8103 (Japan)

[d] Dr. K. Yoshida, Prof. S. Isoda
Institute for Chemical Research, Kyoto University
Uji, Kyoto 611-0011 (Japan)

[e] M. Isosomppi, Prof. N. V. Tkachenko, Prof. H. Lemmetyinen
Institute of Materials Chemistry, Tampere University of Technology
P.O. Box 541, FIN-33101 Tampere (Finland)
Fax: (+358) 3-3115-2108
E-mail: nikolai.tkachenko@tut.fi

Supporting information for this article is available on the WWW under http://www.chemeurj.org/ or from the author. Time profile of the absorbance at 420 nm to monitor the place-exchange reaction of H_2PC11MPP with 16-mercaptohexadecanoic acid in toluene (S1), CT absorption of H_2PC11C15MPP and C_{60} in toluene (S2), CT emission of H_2PC11C15MPP and C_{60} in toluene (S3), and the dependence of $\phi_f^0/[\phi_f^0-\phi_f(\mathrm{obsd})]$ on the reciprocal concentration of C_{60} for H_2PC11C15MPP in toluene and in toluene/acetonitrile [2:1 (v/v)] (S4).

Introduction

Synthetic host molecules are attractive targets that provide a basic understanding of molecular recognition. Previous artificial host molecules include cyclophanes,[1] clefts,[2] calixarenes,[3] porphyrins,[4] metal–ligand clusters,[5] amongst others.[6] Although these constructs have provided fundamental information on molecular recognition in host–guest complexes, it has proven to be more difficult to use such host–guest interactions in molecular devices and machines that exhibit photophysical, electrochemical, and photoelectrochemical functions.[7]

An increasing amount of research is being devoted to the development of potentially less expensive types of organic solar cells, including planar heterojunction,[8] dye-sensitization,[9–11] bulk heterojunction,[12,13] and nanorod-polymer solar cells.[14] In particular, considerable attention has been drawn in recent years to the development of bulk heterojunction cells, which possess an interpenetrating network of donor (D) and acceptor (A) molecules in the blend film, to enhance the charge separation efficiency between the D and A molecules. The combination of porphyrin as an electron donor and fullerene as an electron acceptor seems to be a promising candidate because of 1) the high light-harvesting efficiency of porphyrin throughout the solar spectrum, 2) supramolecular complexation between porphyrin and fullerene due to π–π interactions,[15,16] and 3) the efficient production of a long-lived, highly energetic charge-separated state by photoinduced electron transfer (ET) due to the small reorganization energy involved in the ET.[17,18] In this context, we have developed a variety of photovoltaic systems based on supramolecular complexes of porphyrin and fullerene on nanostructured SnO_2 electrodes.[17,19,20] In particular, novel organic solar cells have been prepared by the step-by-step self-organization of porphyrin, C_{60} units and gold nanoparticles on nanostructured SnO_2 electrodes (Route A, Figure 1).[20] At first, porphyrin-alkanethiolate-monolayer-protected gold nanoparticles (H_2PCnMPP, where n is the number of methylene groups in the spacer)[21] were prepared starting from porphyrin-alkanethiol (first step).[22] These porphyrin-alkanethiolate-monolayer-protected gold nanoparticles (MPPs) formed supramolecular complexes with C_{60} molecules in the wedge-shaped holes of the porphyrin MPP (second step) and these further associated into larger composite clusters in an acetonitrile/toluene mixed solvent (third step). Finally, these highly colored composite clusters could be assembled as three-dimensional arrays on nanostructured SnO_2 films to afford a SnO_2 electrode modified with composite clusters of porphyrin and C_{60} molecules by using an electrophoretic deposition method (fourth step).[23] The film of the composite clusters exhibited an incident photon-to-photocurrent efficiency (IPCE) as high as 54%, broad photocurrent action spectra (up to 1000 nm), and a power conversion efficiency of 1.5%, which is much higher than that of reference systems involving a simple combination of porphyrin and C_{60} single components.[20] Although such step-by-step self-organization is potentially useful in the development of organic solar cells, it is still difficult to modulate the three-dimensional morphology of a D–A interpenetrating network by controlling the self-assembly processes of the donor and acceptor molecules.[24]

We report herein a novel approach to the construction of a light–energy conversion system by the supramolecular incorporation of C_{60} molecules into tailored, large and bucket-shaped surface holes on porphyrin MPPs in a mixed solvent, followed by electrophoretic deposition of clusters of these complexes onto nanostructured SnO_2 electrodes (Route B, Figure 1). An exchange reaction of porphyrin alkanethiolates with short-chain alkanethiols in the monolayer of the gold nanoparticles results in the formation of "host" surface holes on porphyrin MPP (H_2PCnCxMPP, where x is the number of methylene groups in the short-chain alkanethiol). In this case, a carboxy group is introduced onto the end of the short-chain alkanethiol so that the surface of the porphyrin MPP exhibits amphiphilic properties, the aim being to suppress undesirable porphyrin MPP aggregation. Thus, we can compare the size and shape effects of the surface holes formed between the porphyrins of the newly developed porphyrin MPP with those of the reference porphyrin MPP, with its small, wedged-shaped surface holes, on the binding of C_{60} molecules. Elucidation of the relationship between the host–guest interactions and the photoelectrochemical function in this system will provide valua-

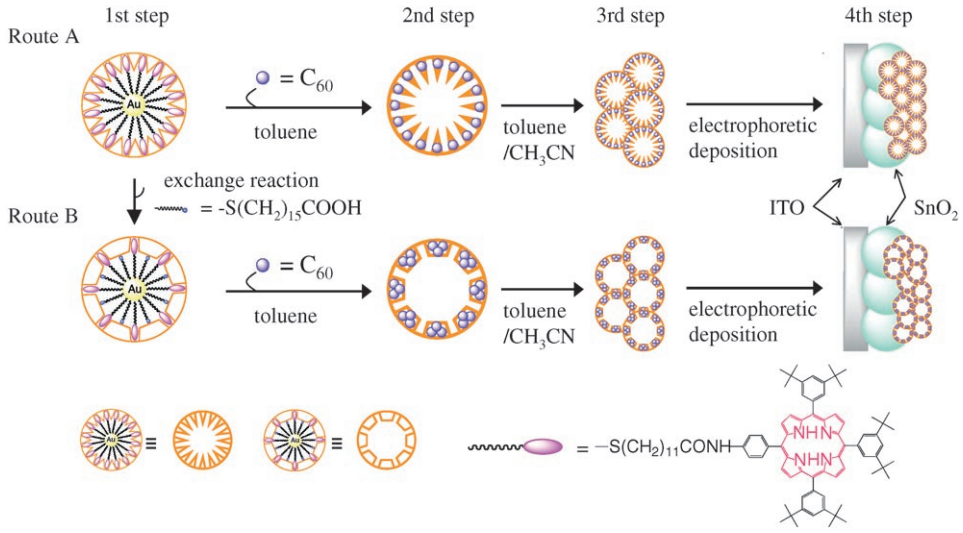

Figure 1. Step-by-step self-organization of porphyrin and C_{60} onto nanostructured SnO_2 electrodes.

ble information for the design of molecular devices and machines including molecular photovoltaics.

Results and Discussion

Supramolecular complexation of porphyrin MPPs and C_{60}: Porphyrin MPP (H_2PC11MPP) was synthesized by following the same method as described previously.[21] Porphyrin-alkanethiol mixed MPP (H_2PC11C15MPP) was then obtained by place-exchange reaction of the porphyrin MPP with 16-mercaptohexadecanoic acid in toluene. The relative ratio of the porphyrin alkanethiolates and the short-chain alkanethiolates on the gold nanoparticles was controlled by varying the reaction time (see the Supporting Information, S1). Porphyrin MPPs, H_2PC11MPP and H_2PC11C15MPP, were purified by gel-permeation chromatography. As expected, H_2PC11C15MPP is soluble in both nonpolar (i.e., toluene, $CHCl_3$, and THF) and polar (i.e., DMF and acetone) solvents, whereas H_2PC11MPP is soluble in only nonpolar solvents. Nonetheless, both types of porphyrin MPPs are insoluble in acetonitrile. This allows us to make composite clusters of the porphyrin MPPs and C_{60} in a toluene/acetonitrile mixture (vide infra). H_2PC11C15MPP was characterized by ^{1}H NMR and UV/Vis spectroscopy, elemental analysis, and transmission electron microscopy (TEM). The mean diameter ($2R_{CORE}$) of the gold core determined by TEM is 2.4 nm with a standard deviation σ of 0.5 nm. By regarding the gold core as a sphere with density ρ_{Au} (58.01 atoms nm^{-3})[25] covered with an outermost layer of hexagonally close-packed gold atoms (13.89 atoms nm^{-3})[25] with a radius of $R_{CORE}-R_{Au}$ ($R_{Au}=0.145$ nm),[25] it can be predicted that the cores of H_2PC11MPP and H_2PC11C15MPP contain 420 gold atoms, of which 194 lie on the gold surface. Given the results of the elemental analysis of H_2PC11C15MPP (H, 5.27; C, 47.50; N, 3.08%), there are 90 porphyrins and 60 short-chain alkanethiolates on the gold surface of H_2PC11C15MPP. Thus, 40% of the porphyrin moieties on the surface of H_2PC11MPP are lost to yield H_2PC11C15MPP, which is expected to incorporate C_{60} molecules into its large, bucket-shaped surface holes (ca. three C_{60} molecules per hole) to form a supramolecular complex.[26] This is in sharp contrast to the previously reported supramolecular complexation between H_2PC11MPP and C_{60}, in which the small, wedge-shaped cavities consisting of two porphyrins bind one C_{60} molecule to form a 1:1 complex.[20]

To shed light on the supramolecular complexation between H_2PC11C15MPP and C_{60}, the absorption spectrum of a mixture of H_2PC11C15MPP ([H_2P] = 0.13 mM) and C_{60} ([C_{60}] = 0.76 mM) in toluene was compared with the sum of the respective spectra of H_2PC11C15MPP ([H_2P] = 0.13 mM) and C_{60} ([C_{60}] = 0.76 mM) in toluene (see the Supporting Information, S2). A charge-transfer (CT) absorption band arising from the π complex formed between the porphyrin and C_{60} appeared at around 650–800 nm[27,28] in the absorption spectrum of the mixture of H_2PC11C15MPP and C_{60} in toluene which was not seen in the sum of the respective absorption spectra of H_2PC11C15MPP and C_{60} in toluene. No appreciable CT band emerged in the absorption spectrum of a mixture of H_2P-ref ([H_2P] = 0.13 mM) and C_{60} ([C_{60}] = 0.76 mM) in toluene, which is similar to the sum of the respective absorption spectra of H_2P-ref and C_{60} in toluene (S2). Thus, the tailored surface holes on the porphyrin MPPs can effectively incorporate C_{60} guest molecules to form a supramolecular complex between H_2PC11C15MPP and C_{60} in toluene.

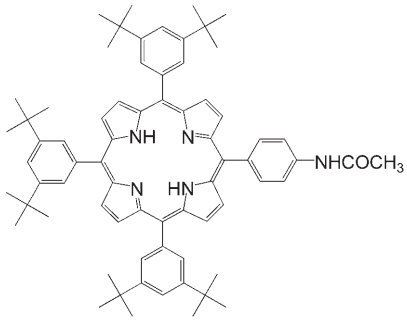

H_2P-ref

A steady-state fluorescence spectrum was recorded for a mixture of H_2PC11C15MPP and C_{60} in toluene ([H_2P] = 0.17 mM, [C_{60}] = 1.00 mM, λ_{ex} = 420 nm). CT emission due to π complexation between the porphyrins and C_{60} molecules is seen at around 800 nm[27,28] for the mixture of H_2PC11C15MPP and C_{60} in toluene, which was not observed in the fluorescence spectrum of H_2PC11C15MPP in the absence of C_{60} in toluene (see the Supporting Information, S3). This demonstrates that H_2PC11C15MPP and C_{60} form tightly packed supramolecular complexes in toluene to exhibit CT emission.

The apparent association constants (K_{app}) for the formation of supramolecular complexes between porphyrin MPPs and C_{60} molecules [Eq. (1) in which α is the degree of association between H_2P and C_{60}[20b]] in toluene and in a mixed solvent (acetonitrile/toluene, 1:2) were determined by analysis of the fluorescence quenching of porphyrin MPPs by C_{60} to estimate the degree of incorporation of C_{60} into the porphyrin MPPs.[20b] The results of the fluorescence quenching experiments are shown in Figure 2. Under the experimental conditions, the fluorescence quenching of the reference system, H_2P-ref, by C_{60} was negligible.[29] On the other hand, in the case of H_2PC11C15MPP and H_2PC11MPP in both toluene and in the mixed solvent, the fluorescence from the porphyrin moiety decreased with increasing C_{60} concentration. In addition, a concomitant increase in the weak CT emission appeared at around 800 nm only in nonpolar toluene (Figure 2a), whereas no appreciable CT emission at 800 nm was seen in the polar mixed solvent (Figure 2b). This behavior can be rationalized by the fact that the intensity of the CT emission decreases with increasing solvent polarity.[27]

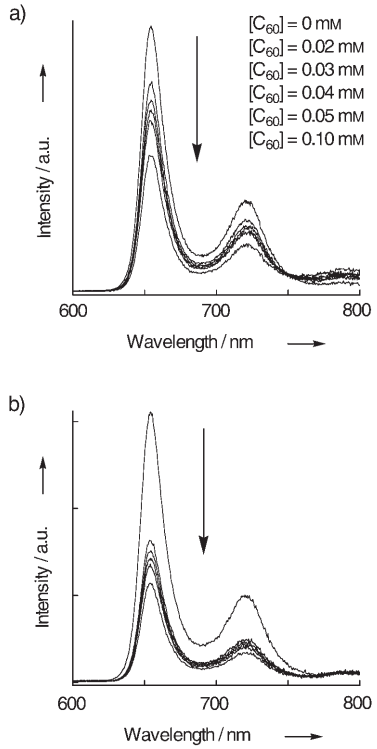

Figure 2. Steady-state fluorescence spectra of a) $H_2PC11C15MPP$ in toluene and b) $H_2PC11C15MPP$ in toluene/acetonitrile (2:1, v/v) at various concentrations of C_{60} ($[H_2P]=5\,\mu M$, $[C_{60}]=0$–$0.10\,mM$, $\lambda_{ex}=435$ nm).

$$\begin{array}{ccccc} H_2P & + & C_{60} & \overset{K_{app}}{\rightleftharpoons} & (H_2P\cdots C_{60}) \\ (1-\alpha)[H_2P] & & [C_{60}]-\alpha[H_2P] & & \alpha[H_2P] \end{array} \quad (1)$$

By using Equation (1), a linear dependence of $1/[\phi_f^0-\phi_f(\mathrm{obsd})]$ on $[C_{60}]^{-1}$ was obtained [Eq. (2), where $\phi_f(\mathrm{obsd})$ is the observed fluorescence quantum yield of H_2P in solution and ϕ_f^0 and ϕ_f' are the fluorescence quantum yields of uncomplexed and complexed molecules of H_2P ($[C_{60}]\gg[H_2P]$)].[20b]

$$\frac{1}{\phi_f^0-\phi_f(\mathrm{obsd})}=\frac{1}{\phi_f^0-\phi_f'}+\frac{1}{K_{app}(\phi_f^0-\phi_f')[C_{60}]} \quad (2)$$

The K_{app} values of $H_2PC11C15MPP$ and $H_2PC11MPP$, as determined from the double reciprocal plots [Eq. (2)], are 2.6×10^4 and $2.6\times10^4\,M^{-1}$ in toluene and 1.2×10^5 and $1.6\times10^5\,M^{-1}$ in the mixed solvent (acetonitrile/toluene, 1:2), respectively (see Figure S4 in the Supporting Information). The K_{app} values in the mixed solvent are larger by one order of magnitude than those in toluene. Strong lyophobic interactions between the porphyrin and C_{60} molecules are responsible for the high complexation between the porphyrin MPPs and the C_{60} molecules in the mixed solvent. The K_{app} values of $H_2PC11MPP$ and $H_2PC11C15MPP$ are virtually the same in toluene and in the mixed solvent. This suggests that the initial, direct complexation between the porphyrin and C_{60} molecules in the surface holes affects the apparent association behavior, resulting in similar K_{app} values in both systems.

Preparation and characterization of composite clusters of porphyrin MPPs and C_{60}: Porphyrin MPPs form supramolecular complexes with C_{60} molecules in toluene and in a mixed solvent (acetonitrile/toluene, 1:2). At high porphyrin and C_{60} concentrations ($[H_2P]=0.17\,mM$, $[C_{60}]=0$–$1.00\,mM$) in the mixed solvent, the resultant supramolecular complexes associate together with additional C_{60} molecules to form larger composite clusters (vide infra).[19,20] The clusters are then attached to nanostructured SnO_2 electrodes by using an electrophoretic deposition method (200 V for 1 min), as reported previously.[19,20] For instance, the formation of $H_2PC11C15MPP$ and C_{60} composite clusters [denoted as $(H_2PC11C15MPP+C_{60})_m$] was achieved by injecting acetonitrile into a mixture of $H_2PC11C15MPP$ and C_{60} in toluene (final ratio of acetonitrile/toluene = 1:2, v/v). The concentration of porphyrin units (per monomer) in these composite clusters was the same in all the experiments {$[H_2P]=0.17\,mM$ in acetonitrile/toluene (1:2)}, whereas the concen-

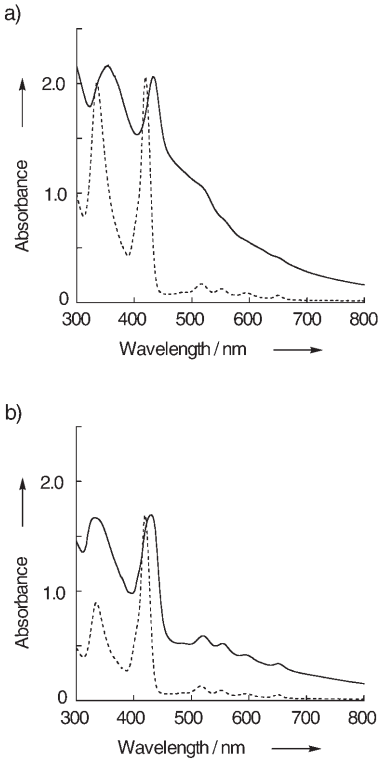

Figure 3. a) Absorption spectrum of $(H_2PC11C15MPP+C_{60})_m$ ($[H_2P]=0.17\,mM$, $[C_{60}]=1.00\,mM$; $[H_2P]:[C_{60}]=1:6$) in acetonitrile/toluene (1:2, v/v) (solid line) and a linear combination of the absorption spectra of $H_2PC11C15MPP$ and C_{60} ($[H_2P]=3.4\,\mu M$, $[C_{60}]=20.0\,\mu M$; $[H_2P]:[C_{60}]=1:6$) in toluene (dotted line). The linear combination was normalized at the Soret band for comparison. b) Absorption spectrum of $(H_2PC11C15MPP+C_{60})_m$ ($[H_2P]=0.17\,mM$, $[C_{60}]=0.51\,mM$; $[H_2P]:[C_{60}]=1:3$) in acetonitrile/toluene (1:2, v/v) (solid line) and a linear combination of the absorption spectra of $H_2PC11C15MPP$ and C_{60} ($[H_2P]=3.4\,\mu M$, $[C_{60}]=10.0\,\mu M$; $[H_2P]:[C_{60}]=1:3$) in toluene (dotted line). The linear combination was normalized at the Soret band for comparison.

tration of C_{60} was varied {$[C_{60}]=0$–1.00 mM in acetonitrile/toluene (1:2)}. This procedure allowed us to achieve complex formation between H_2PC11C15MPP and C_{60} as well as the formation of clusters at the same time. Clusters of H_2PC11MPP and C_{60} [denoted as $(H_2PC11MPP+C_{60})_m$] were also prepared in the same way as a control experiment.

The absorption spectra of $(H_2PC11C15MPP+C_{60})_m$ and $(H_2PC11MPP+C_{60})_m$ in acetonitrile/toluene (1:2) were much broader than those in toluene (Figure 3).[30] The Soret band in the acetonitrile/toluene mixture was red-shifted relative to that in toluene, whereas the positions of the Q-bands were almost the same. These results indicate the formation of clusters in the mixed solvent.[19,20] The broad long-wavelength absorption in the 700–800 nm region is diagnostic of the charge-transfer absorption band that arises as a result of the π complex formed between the porphyrin and C_{60} (vide supra).[27,28] More importantly, the red-shift of the Soret band of $(H_2PC11C15MPP+C_{60})_m$ with a ratio of $[H_2P]:[C_{60}]=1:6$ (Figure 3a) is much larger than that of $(H_2PC11C15MPP+C_{60})_m$ with a ratio of $[H_2P]:[C_{60}]=1:3$ (Figure 3b). This shows that the interaction between the porphyrin and the C_{60} molecules increases as the relative ratio of C_{60} versus porphyrin increases.

The clusters of $(H_2PC11C15MPP+C_{60})_m$ ($[H_2P]:[C_{60}]=1:6$), $(H_2PC11C15MPP)_m$, and $(C_{60})_m$ were characterized using the dynamic light scattering (DLS) method. In toluene, the average diameter of H_2PC11MPP is reported to be ~10 nm, which is consistent with the value determined by molecular modeling.[20] On the other hand, in a mixture of acetonitrile/toluene (1:2), the size distributions of associated clusters of $(H_2PC11C15MPP+C_{60})_m$, $(H_2PC11C15MPP)_m$, and $(C_{60})_m$ were found to be narrow with mean diameters (D_M) of 190 nm for $(H_2PC11C15MPP+C_{60})_m$, 180 nm for $(H_2PC11C15MPP)_m$, and 350 nm for $(C_{60})_m$ (Figure 4). More importantly, the size distribution of clusters of $(H_2PC11C15MPP+C_{60})_m$ increased with increasing incubation time ($t=2$ min, $D_M=190$ nm; $t=5$ min, $D_M=300$ nm; $t=8$ min, $D_M=310$ nm), whereas those of $(H_2PC11C15MPP)_m$ and $(C_{60})_m$ remained virtually the same. These results suggest that in the mixed solvent C_{60} molecules are incorporated into the tailored host space between the porphyrin moieties in the porphyrin-modified gold nanoparticles to form highly organized aggregates.

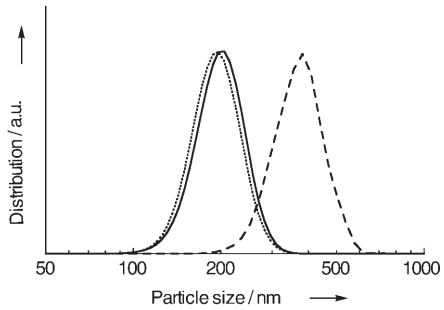

Figure 4. Particle size distribution of $(H_2PC11C15MPP)_m$ (dotted line), $(H_2PC11C15MPP+C_{60})_m$ ($[H_2P]:[C_{60}]=1:6$, solid line), and $(C_{60})_m$ (dashed line) in an acetonitrile/toluene (1:2) mixture at 2 min after injection of acetonitrile into the toluene solutions.

The TEM image of $(H_2PC11C15MPP+C_{60})_m$ (Figure 5a) obtained from drop-casted films of the clusters ($[H_2P]:[C_{60}]=1:6$) on a carbon grid reveals the exclusive formation of rod-like clusters with a well-controlled size (1–2 μm in the long axis and 0.1–0.2 μm in the short axis). In sharp contrast, the TEM images of the clusters of $(H_2PC11C15MPP)_m$ (Figure 5c) and $(C_{60})_m$ (Figure 5d) show ill-defined sizes and shapes. In particular, the TEM image of

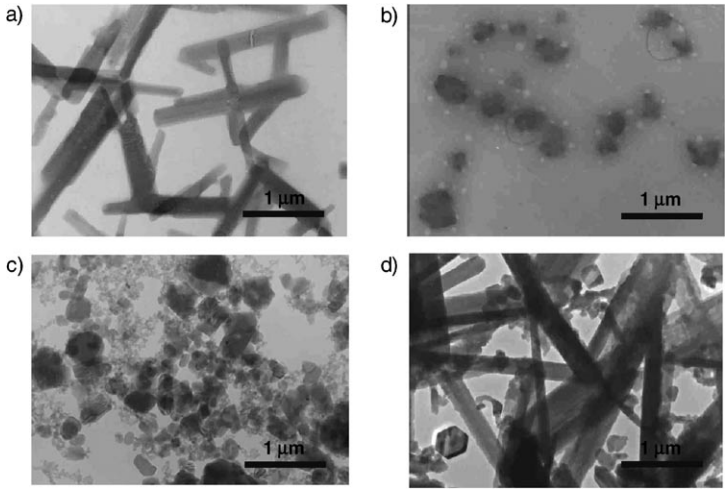

Figure 5. TEM images of a) $(H_2PC11C15MPP+C_{60})_m$ ($[H_2P]=0.17$ mM, $[C_{60}]=1.00$ mM; $[H_2P]:[C_{60}]=1:6$), b) $(H_2PC11C15MPP+C_{60})_m$ ($[H_2P]=0.17$ mM, $[C_{60}]=0.51$ mM; $[H_2P]:[C_{60}]=1:3$), c) $(H_2PC11C15MPP)_m$ ($[H_2P]=0.17$ mM), and d) $(C_{60})_m$ ($[C_{60}]=1.00$ mM). The samples were prepared from the cluster solution in acetonitrile/toluene (1:2), which were evaporated on carbon grids.

clusters of $(C_{60})_m$ reveals both rods of different sizes (1–5 μm in the long axis and 0.1–0.5 μm in the short axis) and small random-shaped structures (0.1–0.5 μm). In addition, variation of the $[H_2P]$:$[C_{60}]$ ratio was found to affect the cluster size and shape (Figure 5a and 5b). The TEM images of $(H_2PC11C15MPP+C_{60})_m$ show that a ratio of $[H_2P]$:$[C_{60}]=1$:6 leads to the formation of well-defined clusters compared with the case of $[H_2P]$:$[C_{60}]=1$:3. This trend is consistent with the size of the large and bucket-shaped surface holes, which are expected to incorporate up to about three C_{60} molecules. A ratio of $[H_2P]$:$[C_{60}]=1$:6 results in the formation of well-defined clusters in which the $H_2PC11C15MPP$ filled with C_{60} molecules further associate with the excess C_{60} molecules to yield composite nanoclusters consisting of alternating arrays of porphyrin and C_{60} covered with C_{60} molecules (vide infra). These results clearly demonstrate that the shape and the size of the surface holes on the $H_2PC11C15MPP$ structure play an important role in controlling the formation of molecular clusters with C_{60} molecules.

To undertake photoelectrochemical measurements, nanostructured SnO_2 electrodes (denoted as ITO/SnO_2) were modified. By subjecting the resultant cluster suspension to a high electric d.c. field (200 V for 1 min), the $(H_2PC11C15MPP+C_{60})_m$ and reference clusters $[(H_2PC11MPP+C_{60})_m]$ were deposited onto the ITO/SnO_2 electrodes to form modified electrodes denoted as ITO/SnO_2/$(H_2PC11C15MPP+C_{60})_m$ and ITO/SnO_2/$(H_2PC11MPP+C_{60})_m$, respectively. The absorptivity of ITO/SnO_2/$(H_2PC11C15MPP+C_{60})_m$ (Figure 6a) was higher than that of ITO/SnO_2/$(H_2PC11C15MPP)_m$ (Figure 6b), and as high as that of ITO/SnO_2/$(H_2PC11MPP+C_{60})_m$.[30] These results show that ITO/SnO_2/$(H_2PC11C15MPP+C_{60})_m$ absorbs most of the incident light in the visible and near-infrared regions. The remarkable broadening of the Soret band in the absorption spectrum of ITO/SnO_2/$(H_2PC11C15MPP+C_{60})_m$ indicates the effective complexation of the porphyrin and C_{60} molecules.[27,28]

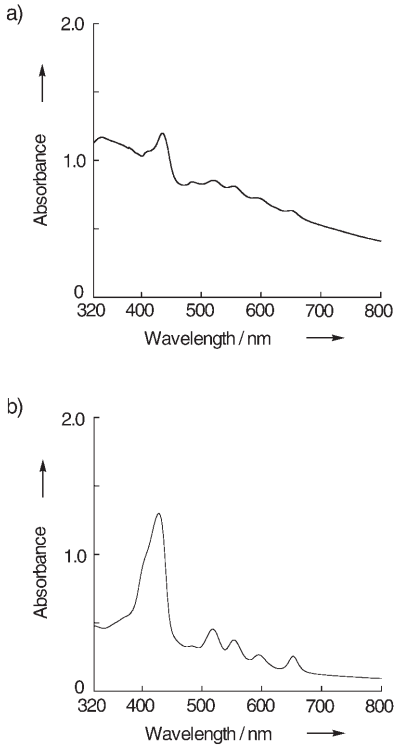

Figure 6. Absorption spectra of a) ITO/SnO_2/$(H_2PC11C15MPP+C_{60})_m$ ($[H_2P]=0.17$ mM, $[C_{60}]=1.00$ mM; $[H_2P]$:$[C_{60}]=1$:6) and b) ITO/SnO_2/$(H_2PC11C15MPP)_m$ ($[H_2P]=0.17$ mM).

The AFM image of ITO/SnO_2/$(H_2PC11C15MPP+C_{60})_m$ reveals the aggregation of a cluster with a size of 200–300 nm (Figure 7a). The cluster size derived from the AFM image is comparable to that determined by the DLS experi-

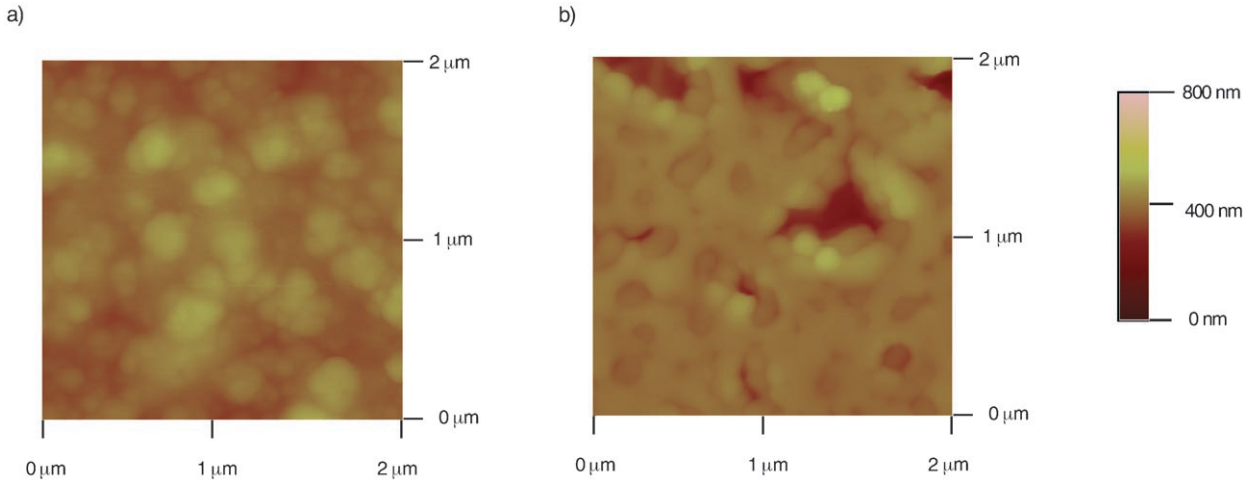

Figure 7. Tapping-mode atomic force micrographs of a) ITO/SnO_2/$(H_2PC11C15MPP+C_{60})_m$ ($[H_2P]=0.17$ mM, $[C_{60}]=1.00$ mM; $[H_2P]$:$[C_{60}]=1$:6) and b) ITO/SnO_2/$(H_2PC11C15MPP)_m$ ($[H_2P]=0.17$ mM) in air. The color scale represents the height topography with bright and dark representing the highest and lowest features, respectively.

ments for composite clusters in acetonitrile/toluene (1:2, v/v) (solid line in Figure 4). On the other hand, the ITO/SnO_2/$(H_2PC11C15MPP)_m$ film exhibits a network structure of viscous, indistinct clusters (Figure 7b). These morphological trends are in good agreement with those obtained from TEM measurements. Note here that because of a high deposition rate, the clusters fail to grow in the form of microcrystallites. Only the slow solvent-evaporation technique employed during the preparation of the TEM grid allows the growth of composite clusters as well-defined microcrystallites. This explains why the rod-like clusters observed in the images of TEM were not found in the AFM images (vide supra).

Comparison of photoelectrochemical properties: Photoelectrochemical measurements were performed with a standard three-electrode system consisting of a working electrode, a platinum wire electrode, and a $Ag/AgNO_3$ reference electrode in a mixture of 0.5 M LiI and 0.01 M I_2 in air-saturated acetonitrile. First, we examined the effect of the concentration of C_{60} on the photoelectrochemical properties of the ITO/SnO_2/$(H_2PC11C15MPP+C_{60})_m$ and ITO/SnO_2/$(H_2PC11MPP+C_{60})_m$ devices at the same applied potential of +0.06 V versus SCE. Under these conditions, an anodic photocurrent passed from the electrolyte solution to the SnO_2 electrode through the cluster films.[19,20,23] The IPCE value of the ITO/SnO_2/$(H_2PC11C15MPP+C_{60})_m$ device increased with increasing C_{60} concentration (0–1.0 mM in acetonitrile/toluene) at a constant concentration of H_2P (0.17 mM) (Figure 8A) and reached a maximum value of 42% at 475 nm ($[H_2P]:[C_{60}]=1:6$). Furthermore, the sample with the highest IPCE value was characterized by a broad photoelectrochemical response spectrum in the visible region (Figure 8A, curve d).[31,32] This indicates that electron transfer from the excited singlet state of porphyrin to C_{60} or the formation of a partial CT state within the supramolecular complex formed between the porphyrin and the C_{60} moieties takes place leading to efficient photocurrent generation.[17,18,27,28] In contrast, the IPCE value of the ITO/SnO_2/$(H_2PC11MPP+C_{60})_m$ device increased initially with increasing C_{60} concentration (0–1.0 mM in acetonitrile/toluene) reaching a maximum of 16% at 440 nm ($[H_2P]:[C_{60}]=1:3$) and then decreased dramatically under the same experimental conditions (Figure 8B). The photocurrent action spectra largely matched the absorption spectra of the SnO_2 electrodes.[31] It should be emphasized here that the IPCE value (42%) of the ITO/SnO_2/$(H_2PC11C15MPP+C_{60})_m$ device with large, bucket-shaped holes is larger by a factor of three than that (16%) of the ITO/SnO_2/$(H_2PC11MPP+C_{60})_m$ device with small, wedge-shaped surface holes on $H_2PC11MPP$. This clearly demonstrates that the shape and size of the host holes on the three-dimensional porphyrin MPP have a large impact on the photoelectrochemical properties. With an excess of C_{60} relative to porphyrin in both the ITO/SnO_2/$(H_2PC11C15MPP+C_{60})_m$ and ITO/SnO_2/$(H_2PC11MPP+C_{60})_m$ devices, an electron produced by photoinduced charge separation between the porphyrin and C_{60} may be relayed through the excess C_{60} molecules to reach the conduction band (CB) of the SnO_2 electrode by an electron-hopping mechanism (vide infra). Thus, depending on the size and the shape of the surface holes on the porphyrin MPPs, the optimal photoelectrochemical conditions in terms of the porphyrin:C_{60} ratio would be different in both devices.

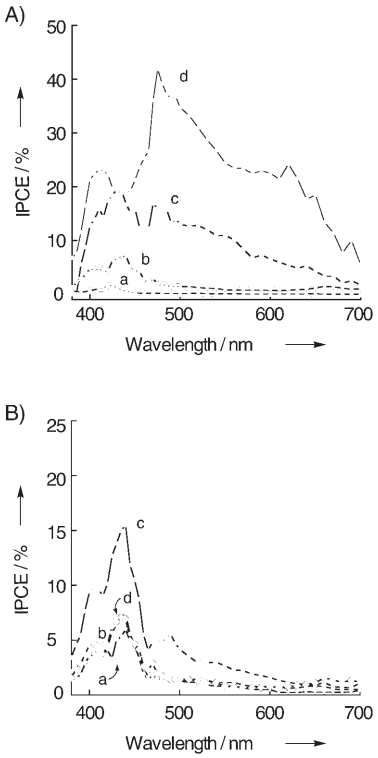

Figure 8. The photocurrent action spectra (IPCE vs. wavelength) of A) ITO/SnO_2/$(H_2PC11C15MPP+C_{60})_m$ and B) ITO/SnO_2/$(H_2PC11MPP+C_{60})_m$ in toluene/acetonitrile (2:1). Potential: +0.06 V versus SCE; electrolyte: 0.5 M LiI and 0.01 M I_2. A) $[H_2P]=0.17$ mM, a) $[C_{60}]=0$ mM (△), b) $[C_{60}]=0.17$ mM ($[H_2P]:[C_{60}]=1:1$, ▽), c) $[C_{60}]=0.51$ mM ($[H_2P]:[C_{60}]=1:3$, □), and d) $[C_{60}]=1.00$ mM ($[H_2P]:[C_{60}]=1:6$, ○). B) $[H_2P]=0.17$ mM, a) $[C_{60}]=0.17$ mM ($[H_2P]:[C_{60}]=1:1$, ▽), b) $[C_{60}]=0.34$ mM ($[H_2P]:[C_{60}]=1:2$, ◇), c) $[C_{60}]=0.51$ mM ($[H_2P]:[C_{60}]=1:3$, □), and d) $[C_{60}]=1.00$ mM ($[H_2P]:[C_{60}]=1:6$, ○).

Ultrafast photodynamics of composite clusters of porphyrin and C_{60} in toluene and in acetonitrile/toluene: The fluorescence lifetimes of the supramolecular complexes formed between porphyrin MPPs and C_{60} in toluene and the composite clusters of the porphyrin MPPs and C_{60} in acetonitrile/toluene (1:2) were measured using the up-conversion technique at the emission wavelength of 655 nm (due to the porphyrin moiety) with excitation at 410 nm, as shown in Figure 9. The decay curves of the fluorescence intensity could be fitted as single or double exponentials. The decay profile for $H_2PC11C15MPP$ in toluene is mono-exponential with a time constant of 90 ps (Figure 9a), which could be attributed to the energy-transfer quenching of the porphyrin excited singlet state by the gold nanoparticle.[21] The addition of C_{60} to $H_2PC11C15MPP$ in toluene led to intensive

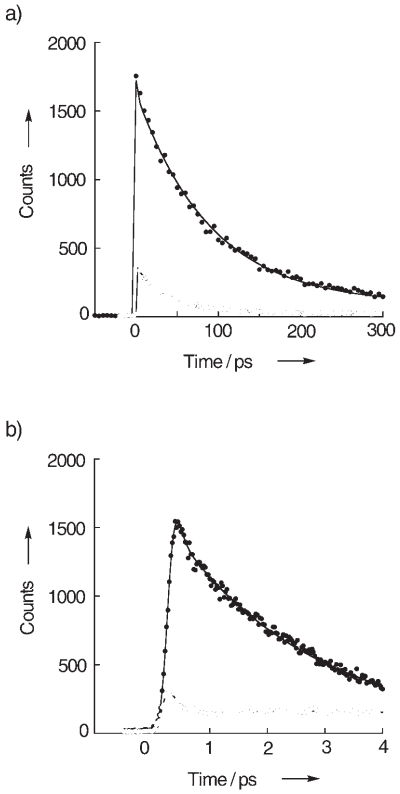

Figure 9. Fluorescence decay curves at 655 nm ($\lambda_{ex}=410$ nm) for a) $H_2PC11C15MPP$ [●, $\tau_1=90$ ps (100%)] and $H_2PC11C15MPP$ and C_{60} [○, $\tau_1=31$ ps (85%), $\tau_2=206$ ps (15%)] ($[H_2P]=0.17$ mM, $[C_{60}]=1.00$ mM; $[H_2P]$:$[C_{60}]=1:6$) in toluene and b) $(H_2PC11C15MPP)_m$ [●, $\tau_1<100$ fs (82%), $\tau_2=2.4$ ps (18%)] and $(H_2PC11C15MPP+C_{60})_m$ (○, $\tau_1<100$ fs (80%), $\tau_2=472$ ps (20%)] ($[H_2P]=0.17$ mM, $[C_{60}]=1.00$ mM; $[H_2P]$:$[C_{60}]=1:6$) in toluene/acetonitrile = 2:1 (v/v).

fluorescence quenching of the porphyrin excited singlet state by C_{60} due to the ultrafast CT interaction in the supramolecular complex formed between the porphyrin and C_{60} (vide infra).[27,28] The resultant two decay components [31 (85%) and 206 ps (15%)] may be ascribed to the unquenched porphyrin excited singlet state in different environments. In the mixed solvent, two decay components with time constants of <100 fs (82%) and 2.4 ps (18%) for $(H_2PC11C15MPP)_m$ may result from ultrafast energy migration between the porphyrins in the clusters and the decay processes correlate with vibration relaxation, internal conversion, and self-quenching (Figure 9b).[21,33] Note that the fluorescence intensity of $(H_2PC11C15MPP+C_{60})_m$ ($[H_2P]$:$[C_{60}]=1:6$) in the mixed solvent is much lower than that of $(H_2PC11C15MPP)_m$ in the same solvent. Similar ultrafast quenching was observed for $(H_2PC11MPP+C_{60})_m$ in the mixed solvent as well as for $H_2PC11MPP$ and C_{60} in toluene relative to the reference systems without C_{60}.[21] These results clearly show extremely fast porphyrin fluorescence quenching by C_{60}, either by ultrafast electron transfer (<100 fs) from the singlet excited states of the porphyrins to the C_{60} molecules or by the formation of a partial CT state between the porphyrin and C_{60} molecules in the supramolecular complex. Since such an ultrafast process is beyond the instrument's time resolution of approximately 100 fs, the components of the fluorescence lifetimes of $(H_2PC11C15MPP+C_{60})_m$ in the mixed solvent and of $H_2PC11C15MPP$ and C_{60} in toluene may be due to minor deactivation pathways of the porphyrin excited singlet state.[34]

The ultrafast relaxation of the porphyrin singlet excited state by interaction with C_{60} in the composite cluster in the mixed solvent and on the ITO/SnO_2 electrode was further examined by femtosecond time-resolved transient absorption spectroscopy. Figure 10a and 10b show the transient absorption component spectra of $(H_2PC11C15MPP+C_{60})_m$ and $(H_2PC11C15MPP)_m$ in the mixed solvent, respectively. An intense bleaching due to the porphyrin excited singlet state of $(H_2PC11C15MPP)_m$ was observed at around 650 nm following laser pulse excitation ($\lambda_{ex}=515$ nm), which ensured the direct formation of the porphyrin excited singlet state (Figure 10b). The three decay components obtained by global analysis may also be assigned to ultrafast energy migration between the porphyrins in the clusters and the decay processes correlate with vibration relaxation, internal conversion, and self-quenching.[21,33] In contrast, broad structureless transient absorption component spectra were obtained for $(H_2PC11C15MPP+C_{60})_m$ in the mixed solvent (Figure 10a). By taking into account the ultrafast porphyrin

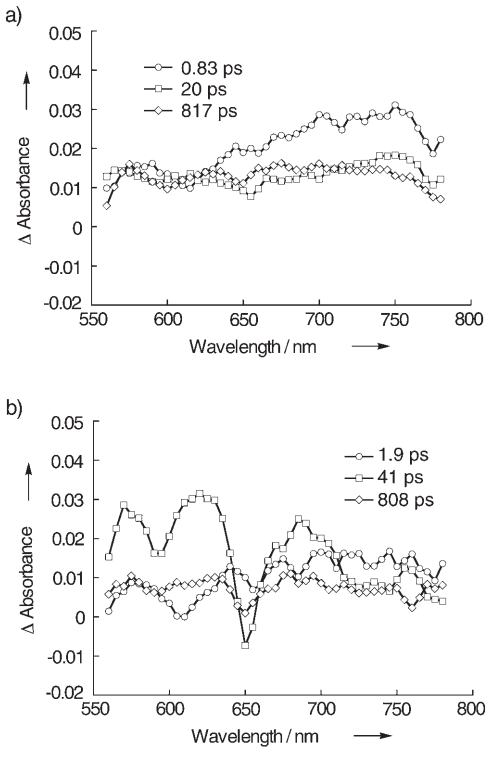

Figure 10. Transient absorption decay component spectra of a) $(H_2PC11C15MPP+C_{60})_m$ ($[H_2P]=0.17$ mM, $[C_{60}]=1.00$ mM; $[H_2P]$:$[C_{60}]=1:6$) and b) $(H_2PC11C15MPP)_m$ ($[H_2P]=0.17$ mM) in toluene/acetonitrile [2:1 (v/v)] obtained by a global three-component fit of the data. The excitation wavelength was 515 nm (the first Q-band of porphyrin). The fitted time constants are displayed on the plots.

fluorescence quenching by C_{60} (<100 fs), the porphyrin excited singlet state is quenched by C_{60} to yield the charge-separated or the partial CT state of the porphyrin and C_{60} molecules. In accordance with this interpretation, the broad transient absorption band in the 700–750 nm region could be assigned to the free-base porphyrin radical cation or the partial CT state,[27,28] whereas no reliable transient absorption spectrum confirming the formation of the C_{60} radical anion was obtained in the 900–1100 nm region[27,28] because of a poor signal-to-noise ratio. Thus, the rapid decay of the bands at 700–750 nm from 0.83 to 20 ps may be attributable to the decay of the free-base porphyrin radical cation or the CT state. The decay components (0.83, 20, and 817 ps) of the transient absorption of $(H_2PC11C15MPP+C_{60})_m$ in the mixed solvent may also be rationalized by the deactivation of the partial CT state in different environments or by minor processes after ultrafast charge separation and charge recombination with a time constant of <100 fs.[34]

Photocurrent generation mechanism: Based on the results of the photodynamic and photoelectrochemical properties of the present system, we have proposed a photocurrent generation mechanism, as shown in Figure 11. Photocurrent generation in the present system is initiated by photoinduced charge separation from the porphyrin excited singlet state ($^1H_2P^*/H_2P^{\bullet+}=-0.7$ V versus NHE)[20] to C_{60} ($C_{60}/C_{60}^{\bullet-}=-0.2$ V versus NHE)[20] or by the formation of a partial CT state in the supramolecular complex of porphyrin and C_{60} rather than by direct electron injection into the conduction band (CB) of the SnO_2 (0 V versus NHE)[20] system.[9–11] The reduced C_{60} or the partial CT state then injects an electron directly into the SnO_2 nanocrystallites or the electron is relayed by electron hopping between the C_{60} molecules. On the other hand, the oxidized porphyrin ($H_2P/H_2P^{\bullet+}=1.2$ V versus NHE)[20] undergoes electron-transfer reduction with the iodide ($I^-/I_3^-=0.5$ V versus NHE)[20] in the electrolyte system. The small reorganization energy of porphyrin and C_{60}[17,18] would facilitate the injection of an electron from the porphyrin excited singlet state into the conduction band of SnO_2 and the rapid donation of an electron from the iodide to the porphyrin radical cation, minimizing the unfavorable charge recombination between the porphyrin and C_{60} molecules. The highest IPCE value (42%) in the ITO/SnO_2/$(H_2PC11C15MPP+C_{60})_m$ device was obtained with a large excess of C_{60} over porphyrin ($[H_2P]:[C_{60}]=1:6$), which rationalizes the possible number of C_{60} molecules (~3) that can be incorporated into the large, bucket-shaped surface holes on $H_2PC11C15MPP$. This is in sharp contrast to the photoelectrochemical properties of the ITO/SnO_2/$(H_2PC11MPP+C_{60})_m$ device in which the highest IPCE (16%) value was achieved with a moderate excess of C_{60} relative to porphyrin ($[H_2P]:[C_{60}]=1:3$), which explains the possible number of C_{60} molecules (~1) incorporated into the small, wedge-shaped surface holes on $H_2PC11MPP$. An electron produced by photoinduced charge separation between porphyrin and C_{60} may be relayed through the excess C_{60} molecules to reach the conduction band (CB) of the SnO_2 electrode by the electron-hopping mechanism.

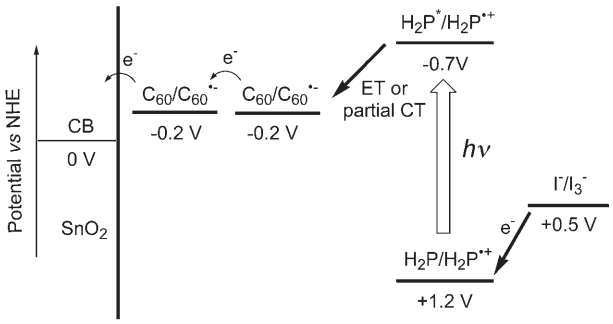

Figure 11. Plausible photocurrent generation mechanism for the ITO/SnO_2/$(H_2PC11C15MPP+C_{60})_m$ device.

Conclusions

In summary, we have successfully disclosed the size and shape effects of surface holes on porphyrin MPP (host)–C_{60} (guest) interactions and their impact on the structure and photoelectrochemical properties of nanostructured SnO_2 electrodes modified with molecular clusters of porphyrin MPP and C_{60} composites. The $H_2PC11C15MPP$ system with large and bucket-shaped holes on the porphyrin MPP has an efficient photoelectrochemical response in the UV/Vis regions compared with the reference $H_2PC11MPP$ system with small and wedge-shaped holes on the porphyrin MPP. The design of such "host" structures on porphyrin MPPs provides a variety of ways to further develop more efficient light–energy conversion systems by modulating the surface structure.

Experimental Section

General methods: Melting points were recorded on a Yanagimoto micro-melting point apparatus and are not corrected. ^{1}H NMR spectra were recorded with a JEOL EX-270 (270 MHz) or a JEOL JMN-AL300 (300 MHz) spectrometer. Elemental analyses were performed at the Microanalytical Laboratory of Kyoto University.

Materials: All solvents and chemicals were of reagent grade quality, obtained commercially, and used without further purification unless otherwise noted (vide infra). $HAuCl_4$ (99.999%) and tetraoctylammonium bromide (98%) were purchased from Aldrich. Tetrabutylammonium hexafluorophosphate (n-Bu_4NPF_6), used as a supporting electrolyte for the electrochemical measurements, was obtained from Tokyo Kasei Organic Chemicals. THF was purchased from Wako Pure Chemical Ind., Ltd. and purified by successive distillation over sodium benzophenone ketyl before use. Thin-layer chromatography (TLC) and flash column chromatography were performed with 25 DC-Alufolien Aluminiumoxid 60 F_{254} Neutral (Merck) and silica gel 60N (Kanto Chemicals), respectively.

Synthesis: Porphyrin MPP ($H_2PC11MPP$) was synthesized by following the same method as described previously.[21] Porphyrin-alkanethiol mixed MPP ($H_2PC11C15MPP$) was then obtained by place-exchange reaction of porphyrin MPP with 16-mercaptohexadecanoic acid in toluene (S1).

Porphyrin MPP ($H_2PC11C15MPP$): 16-Mercaptohexadecanoic acid (10.8 mg, 0.037 mmol) was added to a solution of $H_2PC11MPP$ (50.4 mg)

in toluene (25 mL). After stirring the reaction mixture for 9 h at room temperature under argon in the dark, the solvent was evaporated to dryness. The residue was purified by gel-permeation chromatography (Biobeads S-X1 200–400 mesh, toluene). Reprecipitation with hexane-2-propanol afforded H_2PC11C15MPP as a black purple solid (31.0 mg). Elemental analysis calcd (%) for $(C_{80}H_{100}N_5OS)_{90}(C_{16}H_{31}O_2S)_{60}Au_{420}$: C 47.53, H 5.32, N 3.06; found: C 47.50, H 5.27, N 3.08.

Preparation of clusters and their deposition onto ITO/SnO_2 electrodes: H_2PC11C15MPP, H_2PC11MPP, and C_{60} are readily soluble in nonpolar solvents such as toluene. In mixed solvents, however, they aggregate and form larger clusters. Nanostructured SnO_2 films were cast on an optically transparent indium-tin oxide (ITO) electrode by applying a dilute (1.5%) colloidal solution of SnO_2 (Chemat) and annealing the dried film at 673 K. These films are highly porous and are electrochemically active, being able to conduct charges across the film. The SnO_2 film electrode (ITO/SnO_2) and an ITO plate were introduced into a 1 cm pathlength cuvette and were connected to positive and negative terminals of the power supply, respectively. A known amount (~1.5 mL) of the cluster solution in acetonitrile/toluene (1:2, v/v) was transferred to the cuvette in which the two electrodes (viz., ITO/SnO_2 and ITO) were kept at a distance of about 6 mm by using Teflon spacer. A d.c. voltage (200 V) was applied between these two electrodes for 1 min using a ATTO AE-8750 power supply. Deposition of a film of clusters onto the ITO/SnO_2 electrode can be visibly seen as the solution becomes colorless with simultaneous coloration of the ITO/SnO_2 electrode.

Characterization: The UV/VIS spectra of solutions and films were recorded with a Perkin-Elmer Lambda 900UV/visNIR spectrophotometer. Steady-state fluorescence spectra were acquired with a SPEX FluoroMAX-3 spectrometer and measured with a Fluorolog 3 spectrofluorimeter (ISA Inc.) equipped with a cooled IR-sensitive photomultiplier (R2658). Dynamic light scattering studies were carried out using an Horiba LB-550 instrument. Transmission electron micrographs (TEM) of the clusters were recorded by applying a drop of the sample onto a carbon-coated copper grid. Images were recorded using a JEOL JEM-200CX transmission electron microscope. AFM measurements were carried out by using a Digital Nanoscope III in the tapping mode.

Photoelectrochemical measurements: The photoelectrochemical measurements were performed in a one-compartment Pyrex UV cell (5 mL) with a standard three-electrode system consisting of a working electrode, a platinum wire counter-electrode, and a Ag/$AgNO_3$ reference electrode in 0.5 M LiI and 0.01 M I_2 in acetonitrile as the electrolyte. Photocurrents were measured with an ALS 630A electrochemical analyzer. A monochromatic light generated by shining a 500 W xenon lamp (Ushio XB-50101AA-A) through a monochromator (Ritsu MC-10N) was used for the excitation of the thin films cast on the SnO_2 electrodes. The IPCE values were calculated by normalizing the photocurrent values for incident light energy and intensity and by using the expression IPCE (%) = $100 \times 1240 \times I/(W_{in} \times \lambda)$, where I is the photocurrent, W_{in} is the incident light intensity, and λ is the excitation wavelength.

Spectral measurements: A pump-probe method was used to measure transient absorption spectra in the sub-picosecond to nanosecond time range. The measurements were carried out using the instrument described previously[28] with the addition of an optical parametric amplifier (CDP 2017, CDP Inc., Russia) to generate excitation pulses at 515 nm. The transient spectra were recorded with a CCD detector coupled to a monochromator in the visible and near-IR ranges. A typical time resolution of the instrument was 200–300 fs (FWHM). Emission decays were measured using an up-conversion method as described elsewhere.[28] An excitation wavelength of 420 nm was used with a time resolution of 200 fs (FWHM).

Acknowledgements

This work was supported by Grant-in-Aid (No. 11740352 to H.I.) from MEXT, Japan. H.I. also thanks Grant-in-Aid from MEXT, Japan (21st Century COE of Kyoto University Alliance for Chemistry) for financial support. A part of this work was supported by the "Nanotechnology Support Project" of the Ministry of Education, Culture, Sports, Science and Technology (MEXT), Japan. M.I., N.T., and H.L. thank the Academy of Finland for financial support.

[1] a) T. H. Webb, H. Suh, C. S. Wilcox, *J. Am. Chem. Soc.* **1991**, *113*, 8554; b) R. Meric, J.-P. Vigneron, J.-M. Lehn, *J. Chem. Soc., Chem. Commun.* **1993**, 129; c) S. M. Ngola, D. A. Dougherty, *J. Org. Chem.* **1998**, *63*, 4566; d) S. M. Ngola, P. C. Kearney, S. Mecozzi, K. Russell, D. A. Dougherty, *J. Am. Chem. Soc.* **1999**, *121*, 1192; e) K. Kano, T. Kitae, Y. Shimofuri, N. Tanaka, Y. Mineta, *Chem. Eur. J.* **2000**, *6*, 2705.

[2] a) A. Metzger, V. M. Lynch, E. V. Anslyn, *Angew. Chem.* **1997**, *109*, 911; *Angew. Chem. Int. Ed. Engl.* **1997**, *36*, 862; b) A. Metzger, E. V. Anslyn, *Angew. Chem.* **1998**, *110*, 682; *Angew. Chem. Int. Ed.* **1998**, *37*, 649; c) T. Grawe, T. Schrader, R. Zadmard, A. Kraft, *J. Org. Chem.* **2002**, *67*, 3755; d) K. Niikura, A. Metzger, E. V. Anslyn, *J. Am. Chem. Soc.* **1998**, *120*, 8533; e) M. Rekharsky, Y. Inoue, S. Tobey, A. Metzger, E. V. Anslyn, *J. Am. Chem. Soc.* **2002**, *124*, 14959.

[3] a) J. L. Atwood, L. J. Barbour, P. C. Junk, G. W. Orr, *Supramol. Chem.* **1995**, *5*, 105; b) J.-M. Lehn, R. Meric, J.-P. Vigneron, M. Cesario, J. Guilhem, C. Pascard, Z. Asfari, J. Vicens, *Supramol. Chem.* **1995**, *5*, 97; c) F. Sansone, S. Barboso, A. Casnati, D. Sciotto, R. Ungaro, *Tetrahedron Lett.* **1999**, *40*, 4741; d) G. Arena, A. Contino, T. Fujimoto, D. Sciotto, Y. Aoyama, *Supramol. Chem.* **2000**, *11*, 279; e) S. J. Park, J.-I. Hong, *Tetrahedron Lett.* **2000**, *41*, 8311; f) M. Lazzarotto, F. Sansone, L. Baldini, A. Casnati, P. Cozzini, R. Ungaro, *Eur. J. Org. Chem.* **2001**, 595; g) F. Corbellini, L. D. Costanzo, M. Crego-Calama, S. Geremia, D. N. Reinhoudt, *J. Am. Chem. Soc.* **2003**, *125*, 9946.

[4] a) M. Sirish, H.-J. Schneider, *Chem. Commun.* **1999**, 907; b) R. K. Jain, A. D. Hamilton, *Org. Lett.* **2000**, *2*, 1721; c) T. Mizutani, K. Wada, S. Kitagawa, *J. Am. Chem. Soc.* **2001**, *123*, 6459.

[5] D. L. Caulder, K. N. Raymond, *Acc. Chem. Res.* **1999**, *32*, 975.

[6] a) M. M. Conn, J. Rebek, *Chem. Rev.* **1997**, *97*, 1647; b) J. Rebek, *Acc. Chem. Res.* **1999**, *32*, 278.

[7] V. Balzani, M. Venturi, A. Credi, *Molecular Devices and Machines*, Wiley-VCH, Weinheim, **2003**.

[8] a) C. W. Tang, *Appl. Phys. Lett.* **1986**, *48*, 183; b) P. Peumans, A. Yakimov, S. R. Forrest, *J. Appl. Phys.* **2003**, *93*, 3693; c) B. A. Gregg, *J. Phys. Chem. B* **2003**, *107*, 4688; d) J. Xue, S. Uchida, B. P. Rand, S. R. Forrest, *Appl. Phys. Lett.* **2004**, *84*, 3013.

[9] a) A. Hagfeldt, M. Grätzel, *Acc. Chem. Res.* **2000**, *33*, 269; b) M. Grätzel, *Nature* **2001**, *414*, 338.

[10] C. A. Bignozzi, R. Argazzi, C. J. Kleverlaan, *Chem. Soc. Rev.* **2000**, *29*, 87.

[11] a) N. Hirata, J.-J. Lagref, E. J. Palomares, J. R. Durrant, M. K. Nazeeruddin, M. Grätzel, D. Di Censo, *Chem. Eur. J.* **2004**, *10*, 595; b) P. Piotrowiak, E. Galoppini, Q. Wei, G. J. Meyer, P. Wiewior, *J. Am. Chem. Soc.* **2003**, *125*, 5278; c) P. V. Kamat, M. Haria, S. Hotchandani, *J. Phys. Chem. B* **2004**, *108*, 5166.

[12] a) G. Yu, J. Gao, J. C. Hummelen, F. Wudl, A. J. Heeger, *Science* **1995**, *270*, 1789; b) S. E. Shaheen, C. J. Brabec, N. S. Sariciftci, F. Padinger, T. Fromherz, J. C. Hummelen, *Appl. Phys. Lett.* **2001**, *78*, 841; c) F. Padinger, R. S. Rittberger, N. S. Sariciftci, *Adv. Funct. Mater.* **2003**, *13*, 85; d) M. M. Wienk, J. M. Kroon, W. J. H. Verhees, J. Knol, J. C. Hummelen, P. A. Van Hal, R. A. J. Janssen, *Angew. Chem.* **2003**, *115*, 3493; *Angew. Chem. Int. Ed.* **2003**, *42*, 3371.

[13] a) J. J. M. Halls, C. A. Walsh, N. C. Greenham, E. A. Marseglia, R. H. Friend, S. C. Moratti, A. B. Holmes, *Nature* **1995**, *376*, 498; b) L. Schmidt-Mende, A. Fechtenkötter, K. Müllen, E. Moons, R. H. Friend, J. D. MacKenzie, *Science* **2001**, *293*, 1119; c) J.-F. Nierengarten, *New J. Chem.* **2004**, *28*, 1177; d) J. Xue, B. P. Rand, S. Uchida, S. R. Forrest, *Adv. Mater.* **2005**, *17*, 66; e) T. Tsuzuki, Y. Shirota, J. Rostalski, D. Meissner, *Sol. Energy Mater. Sol. Cells* **2000**, *61*, 1.

[14] a) W. U. Huynh, J. J. Dittmer, A. P. Alivisatos, *Science* **2002**, *295*, 2425; b) J. Liu, T. Tanaka, K. Sivula, A. P. Alivisatos, J. M. J. Fréchet, *J. Am. Chem. Soc.* **2004**, *126*, 6550.

[15] a) H. Imahori, K. Hagiwara, M. Aoki, T. Akiyama, S. Taniguchi, T. Okada, M. Shirakawa, Y. Sakata, *J. Am. Chem. Soc.* **1996**, *118*, 11771; b) D. R. Evans, N. L. P. Fackler, Z. Xie, C. E. F. Rickard, P. D. W. Boyd, C. A. Reed, *J. Am. Chem. Soc.* **1999**, *121*, 8466; c) D. Sun, F. S. Tham, C. A. Reed, L. Chaker, P. D. W. Boyd, *J. Am. Chem. Soc.* **2002**, *124*, 6604; d) K. Tashiro, T. Aida, J.-Y. Zheng, K. Kinbara, K. Saigo, S. Sakamoto, K. Yamaguchi, *J. Am. Chem. Soc.* **1999**, *121*, 9477.

[16] a) T. Yamaguchi, N. Ishii, K. Tashiro, T. Aida, *J. Am. Chem. Soc.* **2003**, *125*, 13934; b) M. Kimura, Y. Saito, K. Ohta, K. Hanabusa, H. Shirai, N. Kabayashi, *J. Am. Chem. Soc.* **2002**, *124*, 5274; c) M. Shirakawa, N. Fujita, S. Shinkai, *J. Am. Chem. Soc.* **2003**, *125*, 9902.

[17] a) H. Imahori, Y. Sakata, *Adv. Mater.* **1997**, *9*, 537; b) H. Imahori, Y. Sakata, *Eur. J. Org. Chem.* **1999**, 2445; c) H. Imahori, Y. Mori, Y. Matano, *J. Photochem. Photobiol. C* **2003**, *4*, 51; d) H. Imahori, *Org. Biomol. Chem.* **2004**, *2*, 1425; e) H. Imahori, *J. Phys. Chem. B* **2004**, *108*, 6130; f) H. Imahori, S. Fukuzumi, *Adv. Funct. Mater.* **2004**, *14*, 525.

[18] a) D. Gust, T. A. Moore, A. L. Moore, *Acc. Chem. Res.* **2001**, *34*, 40; b) S. Fukuzumi, D. M. Guldi in *Electron Transfer in Chemistry* (Ed.: V. Balzani), Wiley-VCH, Weinheim, **2001**, Vol. *2*, pp. 270–337; c) M. E. El-Khouly, O. Ito, P. M. Smith, F. D′Souza, *J. Photochem. Photobiol. C* **2004**, *5*, 79.

[19] a) H. Imahori, T. Hasobe, H. Yamada, P. V. Kamat, S. Barazzouk, M. Fujitsuka, O. Ito, S. Fukuzumi, *Chem. Lett.* **2001**, 784; b) T. Hasobe, H. Imahori, S. Fukuzumi, P. V. Kamat, *J. Phys. Chem. B* **2003**, *107*, 12105; c) T. Hasobe, Y. Kashiwagi, M. A. Absalom, J. Sly, K. Hosomizu, M. J. Crossley, H. Imahori, P. V. Kamat, S. Fukuzumi, *Adv. Mater.* **2004**, *16*, 975; d) T. Hasobe, P. V. Kamat, M. A. Absalom, Y. Kashiwagi, J. Sly, M. J. Crossley, K. Hosomizu, H. Imahori, S. Fukuzumi, *J. Phys. Chem. B* **2004**, *108*, 12865.

[20] a) T. Hasobe, H. Imahori, P. V. Kamat, S. Fukuzumi, *J. Am. Chem. Soc.* **2003**, *125*, 14962; b) T. Hasobe, H. Imahori, P. V. Kamat, T. K. Ahn, S. K. Kim, D. Kim, A. Fujimoto, T. Hirakawa, S. Fukuzumi, *J. Am. Chem. Soc.* **2005**, *127*, 1216; c) H. Imahori, A. Fujimoto, S. Kang, H. Hotta, K. Yoshida, T. Umeyama, Y. Matano, S. Isoda, *Adv. Mater.* **2005**, *17*, 1727.

[21] a) H. Imahori, M. Arimura, T. Hanada, Y. Nishimura, I. Yamazaki, Y. Sakata, S. Fukuzumi, *J. Am. Chem. Soc.* **2001**, *123*, 335; b) H. Imahori, Y. Kashiwagi, T. Hanada, Y. Endo, Y. Nishimura, I. Yamazaki, S. Fukuzumi, *J. Mater. Chem.* **2003**, *13*, 2890; c) S. Fukuzumi, Y. Endo, Y. Kashiwagi, Y. Araki, O. Ito, H. Imahori, *J. Phys. Chem. B* **2003**, *107*, 11979; d) H. Imahori, Y. Kashiwagi, Y. Endo, T. Hanada, Y. Nishimura, I. Yamazaki, Y. Aaraki, O. Ito, S. Fukuzumi, *Langmuir* **2004**, *20*, 73.

[22] H. Imahori, H. Norieda, Y. Nishimura, I. Yamazaki, K. Higuchi, N. Kato, T. Motohiro, H. Yamada, K. Tamaki, M. Arimura, Y. Sakata, *J. Phys. Chem. B* **2000**, *104*, 1253.

[23] a) P. V. Kamat, S. Barazzouk, K. G. Thomas, S. Hotchandani, *J. Phys. Chem. B* **2000**, *104*, 4014; b) P. V. Kamat, M. Haria, S. Hotchandani, *J. Phys. Chem. B* **2004**, *108*, 5166; c) P. V. Kamat, S. Barazzouk, S. Hotchandani, K. G. Thomas, *Chem. Eur. J.* **2000**, *6*, 3914.

[24] Gold nanoparticles have been employed to assemble photoactive molecules on the electrode surfaces of photoelectrochemical devices, but the photocurrent generation efficiencies of these systems are much lower than that described in this work: a) T. Akiyama, K. Inoue, Y. Kuwahara, N. Terasaki, Y. Niidome, S. Yamada, *J. Electroanal. Chem.* **2003**, *550*, 303; b) Y. Kuwahara, T. Akiyama, S. Yamada, *Langmuir* **2001**, *17*, 5714; c) P. K. Sudeep, B. I. Ipe, K. G. Thomas, M. V. George, S. Barazzouk, S. Hotchandani, P. V. Kamat, *Nano Lett.* **2002**, *2*, 29; d) K. G. Thomas, P. V. Kamat, *Acc. Chem. Res.* **2003**, *36*, 888; e) P. V. Kamat, *J. Phys. Chem. B* **2002**, *106*, 7729; f) M. Lahav, V. Heleg-Shabtai, J. Wasserman, E. Katz, I. Willner, H. Durr, Y. Z. Hu, S. H. Bossmann, *J. Am. Chem. Soc.* **2000**, *122*, 11480; g) M. Lahav, T. Gabriel, A. N. Shipway, I. Willner, *J. Am. Chem. Soc.* **1999**, *121*, 258.

[25] R. H. Terrill, T. A. Postlethwaite, C.-h. Chen, C.-D. Poon, A. Terzis, A. Chen, J. E. Hutchison, M. R. Clark, G. Wignall, J. D. Londono, R. Superfine, M. Falvo, C. S. Johnson, Jr., E. T. Samulski, R. W. Murray, *J. Am. Chem. Soc.* **1995**, *117*, 12537.

[26] The possible number of C_{60} molecules (n_F) incorporated into the bucket-shaped surface holes on H_2PC11C15MPP was determined by CPK modeling with the CAChe 4.1 package. By assuming that H_2PC11C15MPP is spherical, the volume of the outermost surface layer including the porphyrin moieties and the bucket-shaped surface holes (the outside radius = 49 Å, the inside radius = 35 Å) was estimated to be 3.1×10^5 Å^3 ($=V_0$). The total volume of the bucket-shaped surface holes [1.1×10^5 Å^3 ($=V_2$)] was obtained by subtracting that of the porphyrin moieties [2.0×10^5 Å^3 ($=V_1$)] from V_0. The n_F value (3.2) was determined by dividing V_2 by the number of the porphyrins per H_2PC11C15MPP (90) and the volume of one C_{60} molecule (380 Å^3).

[27] a) N. Armaroli, G. Marconi, L. Echegoyen, J. P. Bourgeois, F. Diederich, *Chem. Eur. J.* **2000**, *6*, 1629; b) H. Imahori, N. V. Tkachenko, V. Vehmanen, K. Tamaki, H. Lemmetyinen, Y. Sakata, S. Fukuzumi, *J. Phys. Chem. A* **2001**, *105*, 1750; c) N. V. Tkachenko, C. Guenther, H. Imahori, K. Tamaki, Y. Sakata, S. Fukuzumi, H. Lemmetyinen, *Chem. Phys. Lett.* **2000**, *326*, 344; d) V. Vehmanen, N. V. Tkachenko, H. Imahori, S. Fukuzumi, H. Lemmetyinen, *Spectrochim. Acta, Part A* **2001**, *57*, 2229; e) D. M. Guldi, C. Luo, M. Prato, A. Troisi, F. Zerbetto, M. Scheloske, E. Dietel, W. Bauer, A. Hirsch, *J. Am. Chem. Soc.* **2001**, *123*, 9166.

[28] a) N. V. Tkachenko, L. Rantala, A. Y. Tauber, J. Helaja, P. H. Hynninen, H. Lemmetyinen, *J. Am. Chem. Soc.* **1999**, *121*, 9378; b) T. J. Kesti, N. V. Tkachenko, V. Vehmanen, H. Yamada, H. Imahori, S. Fukuzumi, H. Lemmetyinen, *J. Am. Chem. Soc.* **2002**, *124*, 8067; c) N. V. Tkachenko, H. Lemmetyinen, J. Sonoda, K. Ohkubo, T. Sato, H. Imahori, S. Fukuzumi, *J. Phys. Chem. A* **2003**, *107*, 8834.

[29] The results on the reference system rule out the possibility of reabsorption of the porphyrin emission from C_{60} and intermolecular photoinduced processes under the present experimental conditions: N. Armaroli, F. Diederich, L. Echegoyen, T. Habicher, L. Flamigni, G. Marconi, J.-F. Nierengarten, *New J. Chem.* **1999**, *23*, 77; F. Diederich, L. Echegoyen, M. Gómez-López, R. Kessinger, J. F. Stoddart, *J. Chem. Soc., Perkin Trans. 2* **1999**, 1577.

[30] The absorption spectra of the clusters in toluene/acetonitrile mixtures and in ITO substrates (vide infra) may include the scattering of the monitoring light by the micrometer-sized particles.

[31] The action spectrum of the ITO/SnO_2/(H_2PC11C15MPP + C_{60})$_m$ devices with a relative ratio of [H_2P]:[C_{60}] = 1:6 is different to the action spectra of the device with a ratio of [H_2P]:[C_{60}] < 1:3 and the absorption spectra of SnO_2/ITO. The action spectrum may result from a CT interaction between the porphyrin and C_{60} molecules, which is influenced by the relative ratio of the porphyrin and C_{60} molecules as well as by the character of the host structures on the porphyrin MPPs. In addition, the scattering of the incident light by the micrometer-sized particles may also influence the shape of the action spectra. The differences in shape and peak positions of the absorption spectra of SnO_2/ITO and the action spectra may also result from differences between the absorption spectra obtained in the transmission mode in air and the action spectra obtained under photoelectrochemical conditions.

[32] The thickness of the porphyrin–C_{60} composite layers in ITO/SnO_2/(H_2PC11C15MPP + C_{60})$_m$ could not be changed because of the short period (1 min) of applied voltage used for the electrophoretic deposition.

[33] S. Akimoto, T. Yamazaki, I. Yamazaki, A. Osuka, *Chem. Phys. Lett.* **1999**, *309*, 177.

[34] We could not obtain reliable fluorescence lifetimes and transient absorption spectra for the ITO/SnO_2/(H_2PC11C15MPP + C_{60})$_m$ system because of the rapid degradation of the samples under laser illumination.

Received: May 31, 2005
Published online: October 14, 2005

